Vol. 81 No. 3 pp. 510–516 ACTA GEOLOGICA SINICA June 2007

Occurrences of Excess ^{40}Ar in Hydrothermal Tourmaline: Interpretations from ^{40}Ar-^{39}Ar Dating Results by Stepwise Heating

QIU Huaning*, PU Zhiping and DAI Tongmo
Key Laboratory of Isotope Geochronology and Geochemistry, Guangzhou Institute of Geochemistry, Chinese Academy of Sciences, P.O. Box 1131, Guangzhou, Guangdong 510640

Abstract: The occurrences of excess ^{40}Ar within a hydrothermal tourmaline is discussed in term of the analysis data of syngenetic muscovite and tourmaline from the Lushui hydrothermal tin-tungsten deposit in western Yunnan, China, using the ^{40}Ar-^{39}Ar stepwise heating technique. About 80% excess ^{40}Ar was released in the last step when the tourmaline was fused, corresponding to a release of only ~3% ^{39}Ar (K), which indicates that most excess ^{40}Ar was held in the mineral lattice rather than in the channels parallel to the *Z*-axis. This suggests that the excess ^{40}Ar was incorporated during crystallization and not diffused into the tourmaline during the post-crystallization history.

Key words: excess ^{40}Ar, tourmaline, ^{40}Ar-^{39}Ar stepwise heating, hydrothermal tin-tungsten deposit, Yunnan

1 Introduction

It is widely accepted that some excess ^{40}Ar is held in many minerals containing only trace or low amounts of potassium, such as beryl, cordierite, tourmaline, quartz and so on. Where is the majority of the excess argon held? Many researchers emphasized the similarities in the structures of beryl, cordierite and tourmaline, each being based on the six-membered tetrahedron rings (hexagonal rings) which are stacked to yield a series of channels parallel to the *Z*-axis, and believed that the majority of the excess ^{40}Ar was held in the channels (Damon and Kulp, 1958; Dalrymple and Lanphere, 1969; York and Farquhar, 1972). Two possible explanations exist: either the argon was incorporated at the time of crystallization of these minerals, or the argon has diffused into them during their post-crystallization history (York and Farquhar, 1972). The latter is based on that many minerals could not retain argon during their early high-temperature existence. Only after the temperature had dropped below the "blocking temperature" for a particular mineral, the argon retention commenced effectively.

Lanphere and Dalrymple's early studies on samples known to contain excess ^{40}Ar revealed a typical age spectrum pattern that become known as a "saddle-shaped" age spectrum (Lanphere and Dalrymple, 1971; Lanphere and Dalrymple, 1976). They noted that the minimum in the saddle could approach, and presumably attain in certain cases, a geologically meaningful age. Because of the presence of excess ^{40}Ar and scarcity of K, tourmaline has rarely been selected as a K-Ar or ^{40}Ar-^{39}Ar dating mineral. Villa (1990) reported a strongly discordant ^{40}Ar-^{39}Ar spectrum on tourmaline which did not allow a chronological interpretation. While Andriessen et al. (1991) reported the results of a feasibility study on the use of the tourmaline K-Ar system for geochronometry, which showed that all tourmaline from young Alpine leucocratic veins had been crystallized without any inheritance of "old" radiogenic Ar and suggested a high closure temperature for the K-Ar tourmaline system.

The ^{40}Ar-^{39}Ar stepped heating technique makes it possible to release separately the argons held in different locations by heating the irradiated minerals from low to high temperatures step by step. If the true age of a mineral with excess ^{40}Ar is already determined, the occurrences of excess ^{40}Ar can be interpreted according to the release pattern curves of the argon isotopes from the irradiated mineral during the ^{40}Ar-^{39}Ar heating experiment.

The following mineralogical data of the tourmaline group are important for us to discuss the ^{40}Ar-^{39}Ar dating results, which are from the website of "mindat.org" (http://www.mindat.org/min-4003.html):

The general formula for the tourmaline group may be written: $AD_3G_6(BO_3)_3[Si_6O_{18}]Y_3Z$, where:

A = Ca, Na, K, or is vacant (large cations);

* Corresponding author. E-mail: qiuhn@gig.ac.cn.

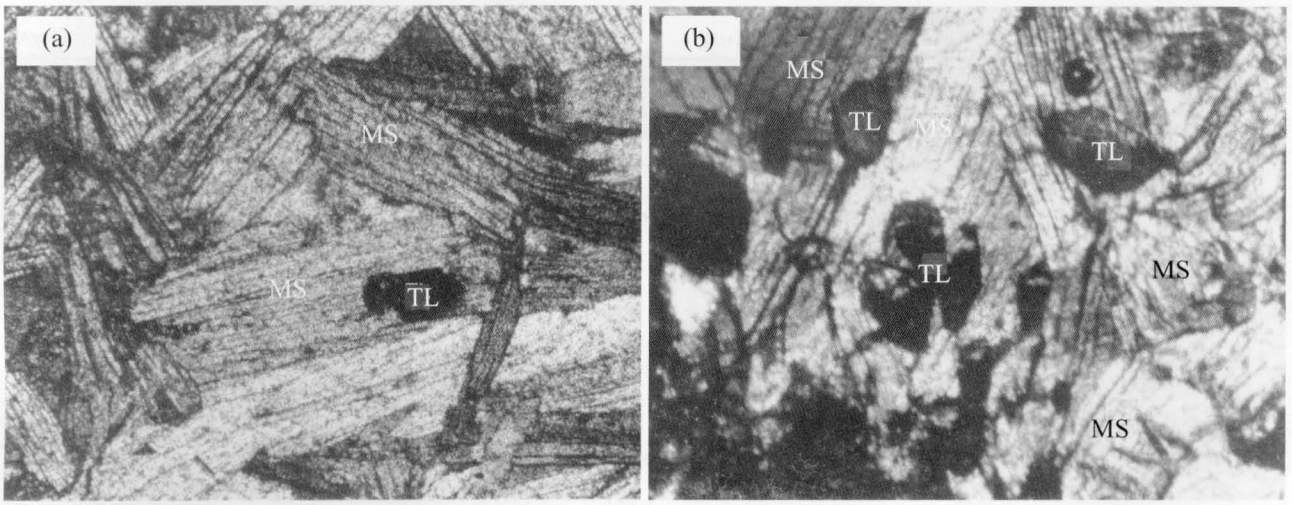

Fig. 1. Photographs showing the syngenetic muscovite (MS) and tourmaline (TL) in S-17.
Orthogonal cross-polarized light, ×55.

D = Al, Fe^{2+}, Fe^{3+}, Li^{+}, Mg^{2+}, Mn^{2+} (intermediate to small cations — in valance balancing combinations when the A site is vacant);

G = Al^{3+}, Cr^{3+}, Fe^{3+}, V^{3+} (small cations);

Y = O and/or OH;

Z = F, O and/or OH.

The structure for the tourmaline group is one in which SiO_4 tetrahedra are linked into six-member rings having a hexagonal pattern and are stacked up with intervening distorted triangular BO_3 groups, linked by D site cations; the SiO_4 tetrahedra are linked vertically by G site cations and Y site anions, while the columns are linked horizontally by both D site cations and Y site anions. The A site cations and the Z site anions occupy the channels down the center of the columns (or the A site may be vacant).

2 Geological Background and Experiments

The muscovite (S-17MS) and tourmaline (S-17TL) within a hand-specimen were selected from a hydrothermal ore vein in the Lushui Tin-tungsten Deposit, western Yunnan, SW China. The muscovite-tourmaline veins (10–30 cm in width) occur along the two sides of a quartz vein (1–2 meters in width), surrounded by the sandy slate rocks of the Hetaoping Formation of the upper Cambrian.

Under the microscope, the phenomena are easy to be observed: small tourmaline (TL) grains locate within a large muscovite (MS) grain or between two MS grains (Fig. 1a and b). These phenomena suggest that the MS and TL crystallized simultaneously from the hydrothermal fluid which formed the tungsten ore veins.

The syngenetic MS and TL grains were separated by hand picking under a binocular microscope and cleaned in an ultrasonic bath. The samples and the monitor standard biotite ZBH-25 (the Chinese K-Ar standard sample from the Fangshan Granodiorite in Beijing with ^{40}Ar-^{39}Ar plateau age of 132.7 ± 0.1 Ma and 7.6% of K) (Wang, 1983; Zhu, 1987) were packed with aluminum laminae and received a neutron fluency of around 4.05×10^{18} n·m^{-2}, and were analyzed by the ^{40}Ar-^{39}Ar stepped heating technique after four months. Argon isotopic ratios were measured on a Micromass® 1200 instrument in the Guangzhou Institute of Geochemistry, Chinese Academy of Sciences. The reactor-derived interferences are corrected with the factors: $(^{36}Ar/^{37}Ar)_{Ca} = 3.2\times10^{-4}$, $(^{39}Ar/^{37}Ar)_{Ca} = 1.08\times10^{-4}$ and $(^{40}Ar/^{39}Ar)_{K} = 8.7\times10^{-3}$.

The samples were loaded into a new molybdenum crucible and heated to successively higher temperature by an electron bombardment furnace, each step lasting 45 minutes. The experiment temperatures had been corrected by loading a thermocouple into the new molybdenum crucible before the sample tree was loaded onto the system. The blanks of the extraction and purification system with 45 min at room temperature were about: $^{40}Ar = 2\times10^{-13}$ mol; $^{39}Ar = 1\times10^{-15}$ mol and $^{36}Ar = 6\times10^{-16}$ mol. The released gases were cleaned up by a titanium sponge furnace at 800 ℃ and a titanium sublimation pump, and then were transferred into the mass spectrometer system using charcoal at liquid nitrogen temperature and further purified by two Sorb-AC pumps (non-evaporable getter pumps). The purified gases were analyzed by the Micromass® 1200 mass spectrometer for the argon isotopic ratios.

3 Results and Discussion

The ^{40}Ar-^{39}Ar dating data by stepped heating are listed in Table 1.

Table 1 ^{40}Ar-^{39}Ar dating data by stepped heating

Step	Temp (°C)	^{36}Ar (± 2σ)	$^{37}Ar_{Ca}$ (± 2σ)	$^{38}Ar_{Cl}$ (± 2σ)	$^{39}Ar_K$ (± 2σ)	^{40}Ar (± 2σ)	$^{40}Ar^*/^{39}Ar_K$ (± 2σ)	^{39}Ar (%)	Age (Ma) (±2σ)	$^{37}Ar_{Ca}/^{39}Ar_K$	$^{40}Ar^*$ (%)
(a) S-17MS, Weight = 0.0578g, J = 0.001495											
1	500	121.11	1175.05	182.72	357.09	26593		0.35		3.29	
		5.66	70.07	5.49	6.70	27					
2	600	299.65	4372.14	614.72	1932.23	67254		2.24		2.26	
		6.02	68.39	5.53	12.96	58					
3	700	682.10	1420.80	276.23	940.02	190227		3.16		1.51	
		6.27	69.23	6.76	6.65	119					
4	800	1132.84	640.10	292.89	3357.05	409490	22.28	6.45	59.1	0.19	18.3
		6.57	72.22	6.91	7.00	549	0.74		2.0		
5	900	768.08	502.94	529.75	17637.70	674102	25.35	23.74	67.1	0.03	66.3
		5.56	62.69	6.08	13.23	820	0.37		1.0		
6	1000	238.67	396.64	839.03	36732.87	1038737	26.35	59.73	69.7	0.01	93.2
		6.53	84.10	5.70	10.52	198	0.37		1.0		
7	1100	226.51	257.18	806.65	34866.41	992227	26.52	93.90	70.2	0.01	93.3
		6.98	69.62	5.38	36.14	468	0.37		1.0		
8	1200	71.32	277.76	221.41	4659.05	137323	24.95	98.46	66.1	0.06	84.7
		4.96	50.10	4.73	9.68	80	0.48		1.3		
9	fused	85.01	116.59	228.43	1570.35	61983	23.47	100.00	62.2	0.07	59.5
		6.31	84.73	7.00	6.51	48	1.22		3.3		
(b) S-17TL, Weight = 0.5459 g, J = 0.001495											
1	500	18.92	11.70	17.93	10.93	8549	271.03	0.37	613.7	1.07	34.6
		0.60	12.09	0.63	1.12	3	73.17		187.3		
2	600	115.05	61.24	31.66	32.28	52634	578.63	1.47	1124.5	1.90	35.4
		0.64	9.67	0.62	0.64	52	21.81		57.9		
3	700	24.92	235.98	26.49	93.58	15600	88.50	4.66	224.2	2.52	52.8
		0.77	10.36	0.60	0.92	11	2.94		7.9		
4	750	16.40	243.34	24.77	201.05	9855	25.05	11.51	66.3	1.21	50.8
		0.52	8.73	0.67	0.56	12	0.82		2.2		
5	800	11.35	223.99	20.05	268.23	7772	16.55	20.64	44.1	0.84	56.8
		0.75	10.05	0.76	0.92	5	0.85		2.3		
6	850	9.61	336.20	16.36	259.67	7887	19.58	29.48	52.1	1.30	64.0
		0.65	9.84	0.64	0.76	6	0.78		2.1		
7	900	11.60	830.39	19.07	331.90	15764	37.50	40.79	98.4	2.50	78.3
		0.60	7.56	0.59	1.69	7	0.78		2.1		
8	950	32.45	1893.74	49.97	873.80	60372	58.45	70.54	151.1	2.17	84.1
		0.54	10.57	0.68	10.78	40	1.15		3.1		
9	1000	8.30	477.27	27.51	456.58	17793	33.73	86.09	88.8	1.05	86.2
		0.58	8.53	0.60	0.91	18	0.59		1.6		
10	1100	10.14	369.41	26.00	309.11	20281	56.10	96.62	145.3	1.20	85.2
		0.60	9.46	0.49	1.01	8	0.96		2.6		
11	fused	55.02	205.97	37.13	99.30	302337	2887.04	100.00	3014.3	2.07	94.6
		1.25	16.10	1.28	1.44	286	9.22		24.7		

(1) Argon isotope concentrations in 10^{-15} moles/g. (2) $^{40}Ar^* = {}^{40}Ar_m - 295.5 \times {}^{36}Ar_m$, m means measured data. (3) ^{37}Ar concentrations have been corrected for decay ($T_{1/2}$ = 35.1 days).

3.1 S-17MS

The cleavages of the muscovite S-17MS are straight under microscope, which shows that it was not affected by the dynamic metamorphism during the Himalayan Period. The age spectrum of the muscovite S-17MS is flat with a plateau age of 68.8 ± 1.1 Ma (2σ, over 93% of the total ^{39}Ar release, Fig. 2). Its isochron age is 68.6 ± 0.5 Ma. So the muscovite formed in ca. 69 Ma ago.

The $^{40}Ar/^{36}Ar$ ratios of the first three steps, 219.6 to 278.9, are well below the atmosphere ratio (295.5) with high Ca/K ratios (Table 1). The interfering reaction of $^{40}Ca(n, n\alpha)^{36}Ar$ during irradiation is only a minor factor and not responsible for the unexpected low $^{40}Ar/^{36}Ar$ ratios. We have no good idea to interpret for this fact at present.

3.2 S-17TL

The age spectrum of the tourmaline S-17TL appears bi-concave (two-saddle-shaped), that is, it starts with high apparent age of 1124 Ma (only 1.5% of ^{39}Ar were released in the first two steps of 500 °C–600 °C), and falls down successively to 44 Ma at step 5 (800 °C), and then rises to a high age of 151 Ma at step 8 (950 °C). Afterwards it falls and rises again, and at the last step (fused) it reaches the highest age of 3014 Ma (Fig. 2a). The total age is 355 ± 14 Ma. The high ages and the total age are much higher than the age of the syngenetic muscovite. Therefore, the tourmaline contains a great deal of excess ^{40}Ar inside.

Calcium and potassium are present in tourmaline. In term of the mineral data, most of the Ca and K are located above the hexagonal rings, that is to say, within the channels parallel to the *Z*-axis. During irradiation, ^{37}Ar

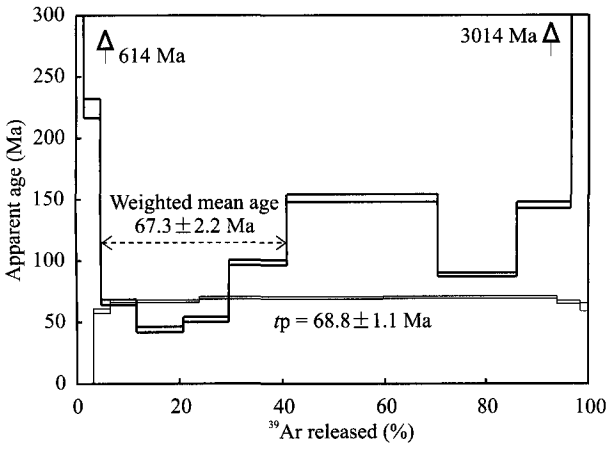

Fig. 2. ^{40}Ar–^{39}Ar age spectra of S-17MS (fine lines) and S-17TL (coarse lines).

The age spectrum of S-17MS is flat with plateau age of 68.8 ± 1.1 Ma. That of S-17TL displays bi-concave with much higher total age of 355 ± 14 Ma and apparent age of 3014 ± 25 Ma in the last step than the plateau age of 68.8 Ma of the syngenetic muscovite S-17MS, showing a great deal of excess ^{40}Ar within the tourmaline sample.

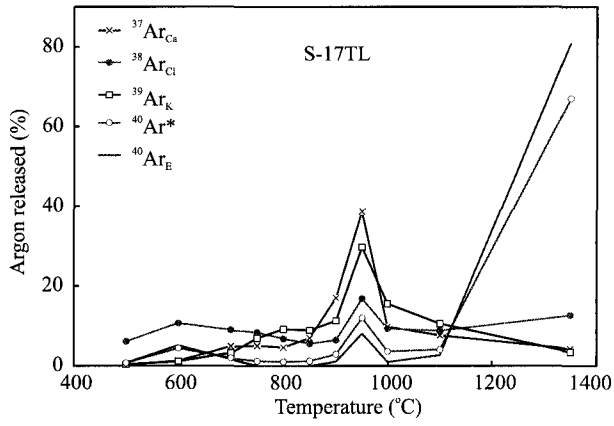

Fig. 3. Plot of argon isotopic releases of S-17TL vs. the heating temperature (°C).

K and Ca were located in the channels parallel to the *Z*-axis, so the highest peaks of ^{39}Ar and ^{37}Ar (950°C) represent the gases from the channels. Only 8% of excess ^{40}Ar was released in step 8 (950°C), and after two higher temperature heating steps (1000°C and 1100°C), 80% of excess ^{40}Ar was released in the last step (1350°C) when the tourmaline sample was fused. Therefore, most of the excess ^{40}Ar cannot be held in the channels but in the mineral lattice (the anion sites or anion vacancies). The three peaks of the excess ^{40}Ar respectively represent the gases released from the fluid inclusions (600°C), the channels (950°C, Z site anions) and the mineral lattice (1350°C, Y site anions).

was induced from $^{40}Ca(n, \alpha)$, ^{38}Ar from $^{37}Cl(n, \gamma)$, and ^{39}Ar from $^{39}K(n, p)$ due to neutron-induced reactions. The release peaks of ^{37}Ar (Ca) and ^{39}Ar (K) would correspond to the gas releases in the sites of the channels parallel to the *Z*-axis. So it can give us important information to infer the occurrences of the excess ^{40}Ar to study the process of argon isotope releases by ^{40}Ar-^{39}Ar step-heating techniques.

The plateau age of 68.8 Ma of the muscovite S-17MS corresponds to a $(^{40}Ar^*/^{39}Ar)_{MS}$ ratio of 26.00. We use this ratio to calculate the radiogenic ^{40}Ar ($^{40}Ar_R$) and the excess ^{40}Ar ($^{40}Ar_E$) within the tourmaline S-17TL for each heating step.

Atmospheric argon:

$^{40}Ar_{air} = 295.5 \times {}^{36}Ar_m$

Radiogenic ^{40}Ar from ^{40}K decay within the tourmaline:

$^{40}Ar_R = {}^{39}Ar_m(^{40}Ar^*/^{39}Ar)_{MS} = 26.00 \times {}^{39}Ar_m$

Excess ^{40}Ar in the tourmaline:

$^{40}Ar_E = {}^{40}Ar_m - {}^{40}Ar_{air} - {}^{40}Ar_R$

$= {}^{40}Ar_m - 295.5 \times {}^{36}Ar_m - 26.00 \times {}^{39}Ar_m$

where subscript m means measured data.

In summary, the excess ^{40}Ar takes up about 67.4% of the total ^{40}Ar release from the tourmaline, and the radiogenic ^{40}Ar 14.7% and the atmospheric ^{40}Ar 17.9%. The fractions of argon isotope releases of the tourmaline S-17TL in each step are listed in Table 2 and shown in Fig. 3, and the correlation coefficients between them are listed in Table 3. The following points are based on these data:

The concentration of K within the tourmaline is 0.36%, calculated with the equation of $K_s=K_{rs}\times (^{39}Ar_K/W)_s/(^{39}Ar_K/W)_{rs}$, where s means the sample (S-17TL) and rs the reference standard sample (ZBH-25).

The correlation coefficient between ^{39}Ar and ^{37}Ar is up to 0.9310 (Table 3) and their release curves are similar (Fig. 3), which express that most K occupy positions equivalent to Ca in the tourmaline.

The very low correlation coefficient between ^{39}Ar and ^{40}Ar indicates that some significant amount of ^{40}Ar was not radiogenic (from the in-situ decay of ^{40}K within the tourmaline S-17TL), but parentless (excess ^{40}Ar).

There are three peaks of excess ^{40}Ar released at 600 °C, 950°C and 1350°C (fused). Three possible corresponding sites holding these excess ^{40}Ar will be

Table 1 Percentages of argon isotope releases of S-17TL

Step	Temp (°C)	^{36}Ar	$^{37}Ar_{Ca}$	$^{38}Ar_{Cl}$	$^{39}Ar_K$	$^{40}Ar^*$ (1)	$^{40}Ar_E$ (2)
1	500	6.03	0.24	6.04	0.37	0.69	0.76
2	600	36.67	1.25	10.66	1.10	4.37	5.09
3	700	7.94	4.83	8.92	3.19	1.94	1.66
4	750	5.23	4.98	8.34	6.85	1.18	–0.06(3)
5	800	3.62	4.58	6.75	9.13	1.04	–0.72(3)
6	850	3.06	6.88	5.51	8.84	1.19	–0.49(3)
7	900	3.70	16.98	6.42	11.30	2.91	1.06
8	950	10.34	38.73	16.83	29.76	11.95	8.02
9	1000	2.65	9.76	9.26	15.55	3.61	0.99
10	1100	3.23	7.56	8.76	10.53	4.06	2.64
11	1350	17.54	4.21	12.50	3.38	67.07	81.05

(1) $^{40}Ar^* = {}^{40}Ar_m - 295.5 \times {}^{36}Ar_m$, m-Valves measured. $^{40}Ar^*$ includes radiogenic and excess ^{40}Ar. (2) Excess ^{40}Ar: $^{40}Ar_E = {}^{40}Ar^* - {}^{39}Ar_m\times (^{40}Ar^*/^{39}Ar)_{MS} = {}^{40}Ar^* - 26.00 \times {}^{39}Ar_m$. (3) A negative figure of excess ^{40}Ar corresponds with an apparent age lower than 68.8 Ma gained from the syngenetic muscovite S-17MS, and the cause is not clear yet.

Table 1 Correlation coefficients between argon isotopes of S-17TL

	^{36}Ar			
$^{37}Ar_{Ca}$	−0.1571	$^{37}Ar_{Ca}$		
$^{38}Ar_{Cl}$	0.4286	0.6413	$^{38}Ar_{Cl}$	
$^{39}Ar_{K}$	−0.3104	0.9310	0.5563	$^{39}Ar_{K}$
^{40}Ar	0.4087	−0.0244	0.5077	−0.1269
$^{40}Ar^{*}$	0.3122	−0.0076	0.4800	−0.0969
$^{40}Ar_{E}$	0.3325	−0.0775	0.4333	−0.1711

$^{38}Ar_{Cl} = {}^{38}Ar_{m} - 0.1869 \times {}^{36}Ar_{m}$; $^{40}Ar^{*} = {}^{40}Ar_{m} - 295.5 \times {}^{36}Ar_{m}$; Excess ^{40}Ar: $^{40}Ar_{E} = {}^{40}Ar^{*} - 26.00 \times {}^{39}Ar_{m}$.

discussed in the following.

The age spectrum of the tourmaline displays extremely steep concentration profiles with initial apparent ages as high as 1124 Ma decreasing to 44 Ma within the first few percent of ^{39}Ar release. The steep profile was probably interpreted to be: (a) excess ^{40}Ar uptake profile that had been frozen into the margins of the mineral crystals following a relatively short interval at high temperature, during which time $^{40}Ar^{*}$ released from minerals lower in the crust resided in the pore space (McDougall and Harrison, 1999); (b) recoil distribution of ^{39}Ar which caused the ratios of $^{40}Ar^{*}/^{39}Ar$ in the margins of mineral crystals higher and so the apparent ages older; (c) excess ^{40}Ar trapped in the fluid inclusions.

Excess ^{40}Ar was trapped within the fluid inclusions of the hydrothermal deposits (Kelley et al., 1986; Qiu and Dai, 1989; Turner and Bannon, 1992; Qiu et al., 1994; Qiu, 1996; Qiu et al., 1997; Qiu et al., 1998; Qiu et al., 2002a, 2002b; Qiu et al., 2003; Qiu and Wijbrans, 2006). At the second step of 600 ℃, small excess ^{40}Ar and $^{38}Ar_{Cl}$ peaks correspond to a lot of ^{36}Ar release (36.7% of the total, Table 2), which shows that most of the fluid inclusions within S-17TL decrepitated at the experiment temperature 600 ℃ in vacuum.

Only 8% of excess ^{40}Ar was released in step 8 (950 ℃) while the releases of ^{39}Ar and ^{37}Ar were at their highest peaks, and after two heating steps (1000 ℃ and 1100 ℃), 80% of excess ^{40}Ar was released in the last step (1350 ℃) when the sample was fused. On the basis of mineralogy, K and Ca were located in the channels parallel to the *Z*-axis, so the highest peaks of ^{39}Ar and ^{37}Ar represent the gases from the channels. Therefore, most of the excess ^{40}Ar should not be contained in the channels but in the mineral lattices (the anion sites or anion vacancies) (Zeitler and Fitz Gerald, 1986). Analogously, most of the excess ^{40}Ar in quartz, beryl, scheelite and albite is released in high heating temperature steps (Qiu et al.,1995; Qiu, 1996; Yu and Mao, 2004; Shen et al., 2005; Wang et al., 2005). This 8% excess ^{40}Ar yields the high apparent age of the step of 950 ℃.

As stated above, most excess ^{40}Ar in the tourmaline was held in the lattice and released in high heating temperature steps, so the excess ^{40}Ar did not diffuse into the tourmaline during post-crystallization history but was incorporated during crystallization.

The weighted mean age for steps 4 to 7 (750 – 900°C) of S-17TL, 67.3 ± 2.2 Ma, is concordant with the plateau age of 68.8 ± 1.1 Ma of S-17MS within the errors. Neither field geological facts nor petrologic observations under microscope show that some minerals formed after the muscovite-tourmaline vein, therefore, the lowest apparent age of 44.1 Ma in step 5 could not be interpreted as a geologically significant age. The lower ages of steps 5 and 6 and the higher age of step 7 might be yielded by the effect of ^{39}Ar recoil during irradiation in the nuclear reactor. The ^{39}Ar recoil caused part of the ^{39}Ar from site A to site B and made the $^{40}Ar^{*}/^{39}Ar$ ratios and the apparent ages rise in site A (900°C) and decrease in site B (850°C and 800°C). This weighted mean age represents a section of gas releases after the fluid inclusions decrepitated and before the gases within channels released and appears to be a reasonable significant age.

Now we summarize here about the occurrences of excess ^{40}Ar within the tourmaline in a few words. The locations of excess ^{40}Ar could be inferred by analyzing the release patterns of the argon isotopes and their correlations from the ^{40}Ar-^{39}Ar dating results by the step-heating technique. The three excess ^{40}Ar peaks at 600, 950 and 1350°C represent respectively the gases released from the fluid inclusions, the channels (Z site anions) and the mineral lattice (Y site anions).

The excess ^{40}Ar in the ore-forming fluid might come from the radiogenic ^{40}Ar of the surrounding rocks and the degasifications of the deep rocks. While the minerals were crystallizing from the fluid in a closed system, the excess ^{40}Ar entered the tourmaline in three main ways: most occupied the locations of the Y site anions, a little part took up the channels and another little part was kept in the fluid inclusions.

3.3 Extraneous ^{40}Ar within (U)HP metamorphic phengite

Extraneous ^{40}Ar is ubiquitous in the (U)HP metamorphic rocks of Dabieshan (Li et al., 1994), the western Alps (Hannula and Mcwilliams, 1995), the Seward Peninsula of Alaska (Scaillet et al., 1992; Arnaud and Kelley, 1995; Ruffet et al., 1995; Scaillet, 1996; Ruffet et al., 1997), the Holsnoy Island of western Norway (Boundy et al., 1997), the Pakistan Himalaya (Tonarini et al., 1993) and the Tavsanli Zone of NW Turkey (Sherlock and Arnaud, 1999; Sherlock and Kelley, 2002).

Two possible sources of extraneous ^{40}Ar exist: (1) inherited ^{40}Ar from protolith (Giorgis et al., 2000); (2) excess ^{40}Ar in the fluid during retrograde metamorphism incorporating into the phengite crystal lattice by diffusion. The inhomogeneous distribution of extraneous ^{40}Ar within the phengite causes the abnormal high ^{40}Ar-^{39}Ar apparent ages and the data point scatter on the isochron diagrams (Qiu and Wijbrans, 2006).

Therefore, the genesis and occurrences of extraneous ^{40}Ar within (U)HP metamorphic phengite might be quite different from those of excess ^{40}Ar within hydrothermal tourmaline in this study.

4 Conclusions

The characteristics of age spectrum and argon isotope releases for the tourmaline S-17TL reveal some major points that we should list here:

(1) The majority of excess ^{40}Ar (~80%) was released when the mineral was fused, which indicates that the excess ^{40}Ar was held in the lattice of the tourmaline.

(2) Only 8% of excess ^{40}Ar was released at the step of the main release peaks of ^{37}Ar (Ca) and ^{39}Ar (K). This fact shows that only a small part of excess was located in the channels parallel to the *Z*-axis.

(3) The excess ^{40}Ar was trapped within the tourmaline lattice during crystallization.

Acknowledgements

We would express our thanks to Prof. Zhang Yuquan and Mr. Chen Hesheng for their kind guides during the fieldwork. We are very grateful to Dr. R. Burgess for his comments and suggestions that significantly improved this work. Financial supports came from the National Natural Science Foundation of China (40472048) and the Chinese Academy of Sciences (KZCX2-SW117 and GIGCX-03-01).

Manuscript received June 9, 2006
accepted Dec. 29, 2006
edited by Xie Guanglian

References

Andriessen, P.A.M., Hebeda, E.H., Simon, O.J., and Verschure, R.H., 1991. Tourmaline K-Ar ages compared to other radiometric dating systems in Alpine anatectic leucosomes and metamorphic rocks (Cyclades and Southern Spain). *Chem. Geol.*, 91(1): 33–48.

Arnaud, N.O., and Kelley, S.P., 1995. Evidence for excess argon during high-pressure metamorphism in the Dora-Maira Massif (western Alps, Italy), using an ultra-violet laser-ablation microprobe ^{40}Ar-^{39}Ar technique. *Contrib. Mineral. Petrol.*, 121(1): 1–11.

Boundy, T.M., Hall, C.M., Li, G., Essene, E.J., and Halliday, A.N., 1997. Fine-scale isotopic heterogeneities and fluids in the deep crust: A $^{40}Ar/^{39}Ar$ laser ablation and TEM study of muscovites from a granulite-eclogite transition zone. *Earth Planet. Sci. Lett.*, 148(1–2): 223–242.

Dalrymple, G.B., and Lanphere, M.A., 1969. Potassium-argon dating. San Francisco: Freeman, 258.

Damon, P.E., and Kulp, J.L., 1958. Excess helium and argon in beryl and other minerals. *Am. Mineral.*, 43: 433–459.

Giorgis, D., Cosca, M., and Li, S.G., 2000. Distribution and significance of extraneous argon in UHP eclogite (Sulu terrain, China): insight from in situ $^{40}Ar/^{39}Ar$ UV-laser ablation analysis. *Earth Planet. Sci. Lett.*, 181(4): 605–615.

Hannula, K.A., and McWilliams, M.O., 1995. Reconsideration of the age of blueschist facies metamorphism on the Seward Peninsula, Alaska, based on phengite $^{40}Ar/^{39}Ar$ results. *J. Metamorphic Geol.*, 13(1): 125–139.

Kelley, S., Turner, G., Butterfield, A.W., and Shepherd, T.J., 1986. The source and significance of argon isotopes in fluid inclusions from areas of mineralization. *Earth Planet. Sci. Lett.*, 79(3–4): 303–318.

Lanphere, M.A., and Dalrymple, G.B., 1971. A test of the $^{40}Ar/^{39}Ar$ age spectrum technique on some terrestrial materials. *Earth Planet. Sci. Lett.*, 12: 359–372.

Lanphere, M.A., and Dalrymple, G.B., 1976. Identification of excess ^{40}Ar by the $^{40}Ar/^{39}Ar$ age spectrum technique. *Earth Planet. Sci. Lett.*, 32: 141–148.

Li, S.G., Wang, S.S., Chen, Y.H., Liu D.L., Qiu, J., Zhou, H.X., and Zhang, Z.M., 1994. Excess argon in phengite from eclogite - evidence from dating of eclogite minerals by Sm-Nd, Rb-Sr and $^{40}Ar/^{39}Ar$ methods. *Chem. Geol.*, 112(3–4): 343–350.

McDougall, I., and Harrison, T.M., 1999. *Geochronology and Thermochronology by the $^{40}Ar/^{39}Ar$ Method* (Second Edition). New York and Oxford: Oxford University Press, 269.

Qiu Hua-Ning and Dai Tong-Mo, 1989. $^{40}Ar/^{39}Ar$ technique for dating the fluid inclusions of quartz from a hydrothermal deposit. *Chinese Sci. Bull.*, 34(22): 1887–1890.

Qiu Hua-Ning and Wijbrans, J.R., 2006. Paleozoic ages and excess ^{40}Ar in garnets from the Bixiling eclogite in Dabieshan, China: new insights from $^{40}Ar/^{39}Ar$ dating by stepwise crushing. *Geochim. Cosmochim. Acta*, 70(9): 2354–2370.

Qiu Hua-Ning, 1996. ^{40}Ar-^{39}Ar dating of the quartz samples from two mineral deposits in western Yunnan (SW China) by crushing in vacuum. *Chem. Geol.*, 127(1–3): 211–222.

Qiu Hua-Ning, Dai Tong-Mo, Pu Zhi-Ping, 1994. Dating mineralization of Lushui Tin-tungsten Deposit, western Yunnan, using ^{40}Ar-^{39}Ar age spectrum technique. *Geochimica*, 23(suppl.): 93–102 (in Chinese with English abstract).

Qiu Hua-Ning, Dai Tong-Mo, Pu Zhi-Ping, 1995. The implications of ^{40}Ar-^{39}Ar saddle-shaped age spectra of trace K minerals from the Lushui Tin-tungsten Deposit, Yunnan Province. *Mineral Deposits*, 14(3): 273–280 (in Chinese with English abstract).

Qiu Hua-Ning, Sun Da-Zhong, Zhu Bing-Quan, and Chang Xiang-Yang, 1997. Isotope geochemistry study of Dongchuan copper deposits in middle Yunnan province, SW China: II. Dating the ages of mineralizations by Pb-Pb and ^{40}Ar-^{39}Ar methods. *Geochimica*, 26(2): 39–45 (in Chinese with English abstract).

Qiu Hua-Ning, Sun Da-Zhong, Zhu Bing-Quan and Chang Xiang-Yang, 1998. ^{40}Ar-^{39}Ar dating for a quartz sample from the Tangdan copper deposit, Dongchuan, Yunnan, by crushing in vacuum and by incremental heating on its powder. *Geochimica*, 27(4): 335–343 (in Chinese with English abstract).

Qiu H. N., Wijbrans J. R., and Li X. H., 2003. ^{40}Ar-^{39}Ar mineralization ages of the Dongchuan-type layered copper deposits, Yunnan, China. *Geochim. Cosmochim. Acta,* 67(18): A386–A386.

Qiu Hua-Ning, Wijbrans J.R., Li Xuan-Hua, Zhu Bing-Quan, Zhu Cong-Lin and Zeng Bao-Cheng, 2002a. New ^{40}Ar-^{39}Ar evidence for ore-forming process during Jinning-Chengjiang period in Dongchuan Type Copper Deposits, Yunnan. *Mineral Deposits*, 21(2): 129–136 (in Chinese with English abstract).

Qiu Hua-Ning, Zhu Bing-Quan and Sun Da-Zhong, 2002b. Age significance interpreted from ^{40}Ar-^{39}Ar dating of quartz samples from the Dongchuan Copper Deposits, Yunnan, SW China, by crushing and heating. *Geochem. J.*, 36(5): 475–491.

Ruffet, G., Feraud, G., Balevre, M., and Kienast, J.R., 1995. Plateau ages and excess argon in phengites — an ^{40}Ar-^{39}Ar laser probe study of Alpine micas (Sesia Zone, western Alps, northern Italy). *Chem. Geol.*, 121(1–4): 327–343.

Ruffet, G., Gruau, G., Ballevre, M., Feraud, G., and Philippot, P., 1997. Rb-Sr and ^{40}Ar-^{39}Ar laser probe dating of high-pressure phengites from the Sesia zone (Western Alps): Underscoring of excess argon and new age constraints on the high-pressure metamorphism.. *Chem. Geol.*, 141(1–2): 1–18.

Scaillet, S., 1996. Excess ^{40}Ar transport scale and mechanism in high-pressure phengites: A case study from an eclogitized metabasite of the Dora-Maira nappe, western Alps. *Geochim. Cosmochim. Acta*, 60(6): 1075–1090.

Scaillet, S., Feraud, G., Ballevre, M., and Amouric, M., 1992. Mg/Fe and (Mg,Fe)Si-Al_2 compositional control on argon behavior in high-pressure white micas - a $^{40}Ar/^{39}Ar$ continuous laser-probe study from the Dora-Maira Nappe of the internal western Alps, Italy. *Geochim.t Cosmochim. Acta*, 56(7): 2851–2872.

Shen Ping, Shen Yuanchao, Zeng Qingdong, Liu Tiebing and Li Guangming, 2005. ^{40}Ar-^{39}Ar age and geological significance of the Sawur Gold Belt in northern Xinjiang, China. *Acta Geologica Sinica* (English Edition), 79(2): 276–285.

Sherlock, S., and Kelley, S., 2002. Excess argon evolution in HP-LT rocks: a UVLAMP study of phengite and K-free minerals, NW Turkey. *Chem. Geol.*, 182(2–4): 619–636.

Sherlock, S.C., and Arnaud, N.O., 1999. Flat plateau and impossible isochrons: Apparent ^{40}Ar-^{39}Ar geochronology in a high-pressure terrain. *Geochim. Cosmochim. Acta,* 63(18): 2835–2838.

Tonarini, S., Villa, I.M., Oberli, F., Meier, M., Spencer, D.A., Pognante, U., and Ramsay, J.G., 1993. Eocene age of eclogite metamorphism in Pakistan Himalaya - Implications for India Eurasia collision. *Terra Nova,* 5(1): 13–20.

Turner, G., and Bannon, M.P., 1992. Argon isotope geochemistry of inclusion fluids from granite-associated mineral veins in southwest and northeast England. *Geochim. Cosmochim. Acta,* 56(1): 227–243.

Villa, I.M., 1990. Geochronology and excess Ar geochemistry of the Lhotse Nup Leukogranite, Nepal-Himalaya. *J. Volcanol. Geothermal Res.*, 44(1–2): 89–103.

Wang Denghong, Mao Jingwen, Yan Shenghao, Yang Jianmin, Xu Jue, Chen Yuchuan and Xue Chunji, 2005. Episodes of Cenozoic gold mineralization on the eastern margin of the Qinghai-Tibet Plateau: $^{40}Ar/^{39}Ar$ dating and implication for geodynamic events. *Acta Geologica Sinica* (English Edition), 79(2): 233–253.

Wang Song-Shan, 1983. Age determinations of ^{40}Ar-^{40}K, ^{40}Ar-^{39}Ar and radiogenic ^{40}Ar released characteristics on K-Ar geostandards of China. *Scientia Geologica Sinica*, (4): 315–321 (in Chinese with English abstract).

York, D., and Farquhar, R.M., 1972. *The Earth's Age and Geochronology*. Oxford: Pergamon Press, 178.

Yu Jinjie and Mao Jingwen, 2004. ^{40}Ar-^{39}Ar dating of albite and phlogopite from porphyry iron deposits in the Ningwu basin in east-central China and its significance. *Acta Geologica Sinica* (English Edition), 78(2): 435–442.

Zeitler, P.K., and Fitz Gerald, J.D., 1986. Saddle-shaped $^{40}Ar/^{39}Ar$ age spectra from young, microstructurally complex potassium feldspars. *Geochim. Cosmochim. Acta,* 50: 1185–1199.

Zhu Jie-Cheng, 1987. Mineralogical characteristics of ZBH-biotite-K-Ar isotopic dating standard sample. *Acta Mineralogica Sinica,* 7(4): 359–365 (in Chinese with English abstract).